Role of DNA polymerases eta, iota and zeta in UV resistance and UV-induced mutagenesis in a human cell line.

Quentin Gueranger, Anne Stary, Saïd Aoufouchi, Ahmad Faili, Alain Sarasin, Claude-Agnès Reynaud, Jean-Claude Weill

ROLE OF DNA POLYMERASES η, ι AND ζ IN UV RESISTANCE AND UV-INDUCED MUTAGENESIS IN A HUMAN CELL LINE.

Quentin Gueranger[1], Anne Stary[2], Saïd Aoufouchi[1], Ahmad Faili[1],

Alain Sarasin[2], Claude−Agnès Reynaud[1] and Jean-Claude Weill[1*].

[1] Institut National de la Santé et de la Recherche Médicale U783 (Développement du Système Immunitaire), Université Paris Descartes, Faculté de Médecine René Descartes, Site Necker-Enfants Malades, 75730 Paris Cedex 15, France.

[2] Centre National de la Recherche Scientifique FRE 2939 (Génomes et Cancers), Institut Gustave Roussy, 94805 Villejuif, France.

Running head: TLS pol specificity in UV-induced damage.

*Address correspondence to J.C. Weill or C.A. Reynaud, INSERM U783, Faculté Necker, 75730 Paris. Tel: +33 1 40 61 53 80 Fax: +33 1 40 61 55 90; E-mail: weill@necker.fr, reynaud@necker.fr

KEYWORDS : Burkitt's lymphoma / translesion / UV damage / Rev3 / cell cycle

ABSTRACT

Genes coding for DNA polymerases η, ι and ζ, or for both Pol η and Pol ι have been inactivated by homologous recombination in the Burkitt's lymphoma BL2 cell line, thus providing for the first time the total suppression of these enzymes in a human context. The UV sensitivities and UV-induced mutagenesis on an irradiated shuttle vector have been analyzed for these deficient cell lines. The double Pol η/ι deficient cell line was more UV sensitive than the Pol η-deficient cell line and mutation hotspots specific to the Pol η-deficient context appeared to require the presence of Pol ι, thus strengthening the view that Pol ι is involved in UV damage translesion synthesis and UV-induced mutagenesis. A role for Pol ζ in a damage repair process at late replicative stages is reported, which may explain the drastic UV-sensitivity phenotype observed when this polymerase is absent. A specific mutation pattern was observed for the UV-irradiated shuttle vector transfected in pol ζ-deficient cell lines, which, in contrast to mutagenesis at the HPRT locus previously reported, strikingly resembled mutations observed in UV-induced skin cancers in humans. Finally, a Pol η PIP-box mutant (without its PCNA binding domain) could completely restore the UV resistance in a Pol η deficient cell line, in the absence of UV-induced foci, suggesting, as observed for Pol ι in a Pol η-deficient background, that TLS may occur without the accumulation of microscopically visible repair factories.

INTRODUCTION

Prokaryotic and eukaryotic cell division implies faithful semi-conservative replication of DNA. On damaged DNA, the replication fork will possibly arrest and call upon a set of specific polymerases whose role is to bypass these lesions so that replication can resume [1].

In humans, ten non-replicative polymerases have been found so far. Among them are the homologues of the yeast Pol ζ along with Rev1, and two homologues of the yeast RAD30 gene products, Pol η and Pol ι. Because there are many TLS polymerases in higher eukaryotes, which have most probably been selected for their mutation avoidance properties, it became attractive to think in

term of cognate interactions [2]. In such a hypothesis, which is supported by several *in vitro* and *in vivo* experiments, each TLS polymerase, alone or with a partner, could bypass a specific group of lesions in an error-free mode.

Exposure of cells to UVC and UVB radiations induces covalent bounds between adjacent pyrimidines, mainly *cis-syn* cyclobutane pyrimidines dimers (CPDs) and less frequently pyrimidine-pyrimidone photoproducts ((6-4) PP). *In vitro*, human Pol η copies CPD T-T dimers like a normal pair of Ts [3, 4] while it is mutagenic opposite the first T of a (6-4) photoproduct and requires Pol ζ to extend from this nucleotide [5] Conversely, Pol ι can insert an A opposite the 3' T of a (6-4) photoproduct while conflicting data have been reported concerning the bypass of CPDs. Two different reports concluded in the inability of Pol iota to cope with such a lesion [6, 7] while the group of R. Woodgate described that Pol iota can perform a mutagenic bypass of CPD [8]. The discrepancies observed between these studies may be in part explained by the differences in the substrate used, notably the nucleotidic sequence surrounding the CPD [9].

The cognate proposition for TLS polymerases was formulated following the *in vivo* situation provided by the variant form of the *xeroderma pigmentosum* (XPV) syndrome. In these patients who display a deficiency in Pol η, there is, despite the presence of a proficient nucleotide excision repair, an increased incidence of UV-induced skin cancers [10, 11]. The best explanation being so far is that another polymerase replaces Pol η in its bypass function but this time in a mutagenic mode.

Yeast Rev3 mutants were isolated based on their deficiency in UV-induced mutagenesis. The *REV3L* gene was found to encode the catalytic subunit of Pol ζ [12] in association with Rev7. It was demonstrated that REV3L was also linked to UV-induced mutagenesis in human cells [12] and UV resistance in avian cells [13]. Strikingly, the human and mouse homologues of Rev3 are twice the size of the yeast protein with a large domain of 1500 amino acids without any homology with yeast Rev3. Inactivation of the *Rev3l* gene in the mouse results in early embryonic lethality, thus suggesting other functions for this enzyme beyond TLS [14-16]. Despite the data collected using purified yeast Rev3 enzyme, the functions of the human and murine REV3L protein remain speculative.

After UV irradiation, Pol ι is targeted to stalled replication forks in association with Pol η and PCNA [17] but there are conflicting data on its role *in vivo*. In a human cell line in which Pol ι expression was down-regulated by siRNA expression, replication of a UV-irradiated shuttle vector

did not reveal any obvious role for this polymerase in TLS and mutagenesis [18]. Pol ι/Pol η double-deficient mice have been analyzed recently by two different groups [19, 20]. In both studies, Pol ι seemed to play a role in the onset of UV-induced skin cancers.

Despite the large number of data obtained mainly from *in vitro* experiments, it remains difficult at this stage to assign a precise role for each TLS polymerase *in vivo*. Moreover, species differences in DNA repair processes and polymerases functions may preclude extending the mouse results to the human situation. By studying human Burkitt's lymphoma BL2 cells in which either Pol η, Pol ι, Pol ζ or both Pol η and Pol ι have been inactivated by homologous recombination, we have been able to collect information on the UV sensitivity and TLS specificities of these different enzymes. This analysis unravels some unique bypass specificities of human Pol ζ and underlines in precise sequence contexts the mutagenic role of Pol ι in a Pol η-deficient background.

EXPERIMENTAL PROCEDURES

Cell line and culture conditions

The type I Burkitt's lymphoma BL2 cell lines were cultured in RMPI 1640 with glutamax (Invitrogen, Carlsbad, CA), supplemented with 10% FCS (Hyclone, Logan, UT) and 100 U/ml penicillin and streptomycin (Invitrogen). The parental BL2 cell line carries the variant *cMYC-IgL* translocation of Burkitt's lymphomas, and has a deficient p53 pathway due to overexpression of its inhibitor, Mdm2 [21].

Inactivation of POLH and REV3L in the BL2 cell line.

All gene inactivations were carried out by transfection of a pBSK vector containing the 5' and 3' gene homologous sequences flanking the antibiotic resistance cassette. Recombination arms (between 2.45 and 3.45 kb) were obtained by amplification of BL2 cells genomic DNA with Pfu polymerase (Stratagene, La Jolla, CA). S-Blasticidin (from pcDNA6/TR), zeocin (from pcDNA4/TO) and histidinol (from pREP 8) resistance genes were cloned from the Invitrogen corresponding plasmids. They were under the control of the SV40 promoter. Hygromycin resistance was driven by a CMV promoter and neomycin resistance by the promoter of the phospho-glycerol kinase gene (*pgk*). Constructs are detailed in fig.1. 10^7 cells were electroporated with 25 μg of linearized targeting vector

and clones selected in 96-wells plates with the appropriate selective agent: G418, 1.5 mg/ml; hygromycin, 350 μg/ml ; zeocin 500 μg/ml; blasticidin, 5 μg/ml; histidinol, 250 μg/ml (all from Invitrogen, except histidinol from Sigma Aldrich). The targeting frequency is around 1% for the first allele and between 0.3 and 0.5 % for the second allele.

Primers used to check homologous recombination at the *POLH* locus are: 3'-KO-eta ACCTGCTTTCTAGTGTCCAG which is located in 3' downstream from the construct and the following primers for each resistance tested: blasti-rev: TTAGCCCTCCCACACATAAC; neo-rev: CACGGGTAGCCAACGC; zeo-rev: CCACGAAGTGCACGCAGTTG and hygro-rev: GGCGAGTACTTCTACACAGC. Primers used to check homologous recombination at the *REV3L* locus: 3'-KO-zeta-1: GCTGTGCTTCAGTGAAGTAC with a hygro-fwd primer GCTGTGTAGAAGTACTCGCC (1st allele) and 3'-KO-zeta-2: CTGTCTATAGGCGGCTTGTG with the neo-rev (2nd allele). Both primers are located in 3' downstream from the construct. K.O. clones were regularly checked to be negative for the amplification of the targeted exons. Pol ι: forward TTCATGATCAAGTGTTGCCC and reverse CTGCCGACTACACTATTCTC. Pol η: forward ATGGTAACACAGTGGCACTG and reverse GACCACAGATGCCATCATTC. REV3L: forward ACAGCAGCCAGAAAGCTATC and reverse GAATGTAACTTCCACATGGGC.

The absence of the REV3L mRNA was checked by RT-PCR (see supplementary fig.1B) using a forward primer located in exon 5 upstream of ATG initiator codon CTTTCTCAGATGGCATTCAG, and a reverse primer located in exon 6 TTTCGGAACTTGACAGCAGC.

EGFP-Pol η constructs and expression

pTet-tTAK-zeo encoding the tetracycline regulated transactivator (gift of T. Honjo) was transfected in the Pol ι and REV3L-deficient BL2 cell lines and pTet-tTAK-neo was transfected in a *POLH*$^{-/-}$ cell line. Wild-type BL2 transfected with pTet-tTAK-zeo was kindly given by T. Honjo. The EGFP was fused to the C-terminal part of Pol η, using pEGFP-C1 vector (Clontech, Mountain View, CA). The EGFP-Pol η fusion protein was cloned into the tetracycline inducible pBI expression vector (Clontech) in which a blasticidin resistance cassette (from pcDNA6/TR, Invitrogen) had been inserted in the Aat II site and the vector obtained was transfected in all transactivated cell lines.

Mutations in the coding sequence of Pol η were generated by PCR mutagenesis on Pol η sequence cloned in pEGFP-C1. The following underlined amino acids were substituted with alanines in the

PIP-box mutant EGFP-Pol η: 702-708: QILESFF. The EGFP-Pol η PIP-box mutant was then cloned in the pIRES puro expression vector. The puromycin is used for selection of transfectants at 350 μg/ml.

UV survival curves and killing assays

$2x10^5$ cells were washed and taken in a 100 μl PBS drop, then irradiated with either UVB or UVC light. UVC light (254 nm) was emitted by a germicidal lamp at a fluence rate of 1 J/m_/s and UVB light (312 nm) was produced by a Bio-sun device (Vilbert Lourmat, Marne-la-Vallée, France) at a fluence rate of 8.3 J/m_/s. After irradiation, cells were incubated for 5 days in complete medium and living cells were counted using Vi-cell XR device (Beckman Coulter, Fullerton, CA).

EGFP-Pol η foci formation after UVC irradiation

EGFP-Pol η positive cells were irradiated using a germicidal lamp at 10 J/m_ at a fluence rate of 1 J/m_/s in 50 μl PBS drops and grown after irradiation in 5 ml of complete medium. Cells were plated after 8 h to 12 h on glass slides using a Cytospin 2 device (Shandon, Waltham MA) prior to fixation with methanol for 10 min at room temperature. Slides were mounted with vectashield® (Abcys, Paris, France) and examined using an Axiovert 200M confocal microscope (Zeiss, Thornwood, NY).

Cell cycle analysis

Cell cycle determination was performed by double staining with propidium iodide (PI) and Bromodeoxyuridine (BrdU). All washing steps were performed with PBT (PBS, BSA 0.5%, Tween 20 0.1%). BrdU 40 μM (Sigma, St Louis, MO) was added to 10^6 cells for 4 h, cells were washed and fixed overnight in 100 μl 70 % ethanol at -20°C. After fixation, DNA was denatured (1ml HCl 2N, Triton® X-100 0.1%) during 20 min at room temperature. Neutralization was performed with sodium tetraborate 0.15 M pH 8.5 during 2 min at room temperature. The anti BrdU FITC antibody was diluted 1/20 (Alexis Biochemicals, San Diego, CA) and incubated with cells for 30 min on ice. Propidium iodide staining was performed in PBS, sodium citrate 0.1%, PI 100 μg/ml at 37°C for 15 min. Analysis was performed using a FACScan cytometer (Becton Dickinson, Franklin Lakes, NJ).

Cell cycle determination after UV irradiation was performed by PI staining on cells synchronized by incubation with 1 mM hydroxyurea during 16h.

Shuttle vector experiment

The SV40-based shuttle vector pR2 carries the 289 bp bacterial *lac*Z' gene and promoter as mutagenesis target, the kanamycin resistance gene, and the SV40 and bacterial replication origins [22]. The pLAS plasmid carries the SV40 T-antigen gene, which is required for replication of the pR2 plasmid. Both vectors were co-transfected by electroporation. After 4 days, all plasmids were recovered using Qiaquick miniprep kit (Qiagen, Valencia, CA), and then digested with *Dpn*I (New England Biolabs, Beverly, MA) to eliminate unreplicated plasmids. The TOP10 *E. coli* strain (Invitrogen) was used for the blue / white screening of *lac*Z' mutants. The pR2 plasmid was irradiated using a Stratalinker 2400 (Stratagene) at 3.5 kJ/m_ at a fluence rate of 25 J/m_/s.

Sequencing was realized on an ABI 3100 sequencer (Applied Biosystems, Foster City, CA) using forward primer: TCGAACACCGAGCGACCCTG.

Hotspots positions on the promoter and coding sequence of the *lac*Z' gene are considered as statistically significant when the occurrence by chance of the observed number of mutations at a given position, related to the total number of mutations collected and to the number of mutable target nucleotides, falls below 1% according to the law of Poisson. For this determination, double close mutations were excluded. Significant hotspots are shown in fig. 6 while total mutations scored are shown in supplementary fig. 3.

Western blot

300 μg of protein were fractionated by SDS PAGE using 10% polyacrylamide gels and transferred on a PVDF Immun-blot™ membrane (Biorad, Hercules, CA). Primary and secondary antibodies were diluted in PBS, Tween 0.02% supplemented with 2.5% BSA and 2.5% dry milk. Polyclonal anti-human Pol η H-300 sc-5592 (1/3000 diluted from Santa Cruz Biotechnology, Santa Cruz, CA), the polyclonal anti-human Pol ι ab1324 (1/4000 diluted from Abcam, Cambridge, UK), the monoclonal anti-PCNA PC10 (1/5000 diluted from Santa Cruz) and the monoclonal anti-c-myc 9E10 sc-40 (1/150 diluted from Santa Cruz) were used. Anti-mouse IgG 170-6516 and anti-rabbit IgG 170-6515 (Biorad), both of them diluted 1/10000, were used as secondary antibodies. Chemoluminescent revelation was made with Westpico ECL (Pierce, Rockford, IL). PCNA ubiquitination was analyzed by SDS PAGE using a 12% polyacrylamide gel and loaded with the triton insoluble fraction. Cells were incubated for 30 sec. in a 1% Triton X-100 PBS and centrifugated, the pellet was subsequently resuspended and sonicated in the loading buffer.

RESULTS

Generation of the polymerase-deficient BL2 cell lines.

Inactivation of the *POLI* gene by homologous recombination in the BL2 cell line has already been described [23]. Two independent clones have been obtained (clones 54 and 267) after successive inactivation of the two alleles. The same strategy was used to inactivate the *POLH* and *REV3L* genes.

$POLH^{-/-}$ cell line

The *POLH* gene was inactivated by replacing exons 2 and 3 by antibiotic resistance genes (fig.1A); exon 2 contains the ATG initiator codon and one of the 5 conserved motifs (DMD) whose mutation abolishes the catalytic activity of yeast Pol η [24]. During the course of this inactivation we observed that the wild-type BL2 cell line has three copies of the *POLH* gene. Although aneuploidies are a common feature of transformed cell lines, a FISH analysis with probes covering over 100 kb of *POLH* failed to reveal any large duplication of the *POLH* locus (data not shown). This small proximal duplication may thus represent a physiological event, as small deletions and duplications have been shown recently to occur rather frequently during normal meiosis [25]. The same constructs with different selection markers were used to inactivate the three alleles. They carry the hygromycin, histidinol and zeocine resistance genes within the *POLH* locus. Three knockout clones, named 123.12, 82.80 and 82.120 in the experiments shown, were derived from two independent heterozygous clones with a $^{-/-/+}$ genotype (82 and 123). *POLH* inactivation was checked by western blot in each of these clones (suppl. fig.1A). Throughout this study, the Pol η-deficient clones are named *$POLH^{-/-}$* for sake of simplicity.

$REV3L^{-/-}$ cell line

We followed the same strategy as the one used by Esposito *et al.* [15] which resulted in embryonic lethality in mice, *i.e.* by replacing exon 5 encoding the ATG initiator codon by resistance cassettes (fig.1B). We inactivated the first allele by deleting 5 kb including exons 5 and 6 and the second allele by deleting 100 bp including exon 5. Two *$REV3L^{+/-}$* clones were obtained and one knockout clone was derived from each heterozygous cell, named 332 and 504 thereafter.

As no human anti-REV3L antibody is available, we checked for the absence of the 5' part of the mRNA in the two clones obtained (suppl. fig. 1B). Moreover, the severity of the phenotype observed on these two independent clones (see below) appears as a good indicator of *REV3L* inactivation.

$POLH^{-/-}$ $POLI^{-/-}$ cell line

We used the same constructs containing histidinol and zeocin resistance genes as the ones used for *POLH* inactivation, and replaced the hygromycin resistance marker by blasticidine in the third construct to transfect the $POLI^{-/-}$ clone 54 (see fig.1A). A single $POLH^{-/-}$ $POLI^{-/-}$ clone was generated in which the inactivation of *POLH* was checked by western blot analysis (supplementary fig.1A).

Characterization of Pol η, Pol ι, Pol η/ι and REV3L-deficient cell lines

The doubling time of exponentially growing cell cultures was checked for each cell line. A slight increase in doubling time for the two single $POLH^{-/-}$ or $POLI^{-/-}$ clones (22h instead of 20h) was reproducibly observed (+/- 30 min), and a more pronounced increase for the $POLH^{-/-}$ $POLI^{-/-}$ clone (24h instead of 20h). $REV3L^{-/-}$ clones showed the largest increase in doubling time (29h).

Cell cycle analysis was performed after 3h of bromodeoxyuridine (BrdU) uptake using propidium iodide and anti-BrdU staining. A similar distribution between the various phases of the cell cycle was observed for the $POLH^{-/-}$, $POLI^{-/-}$, $POLH^{-/-}$ $POLI^{-/-}$ and wild-type cell lines (shown for $POLH^{-/-}$ cells in fig. 2A). On the contrary the REV3L-deficient clones showed a strong accumulation of cells in the G2/M phase (fig. 2A). Furthermore, these clones show increased chromosome abnormalities including breaks, translocations and polyploidy (not shown).

Killing by UV is increased in $POLH^{-/-}$ $POLI^{-/-}$ and $REV3L^{-/-}$ cell lines

The UV-induced cytotoxicity in mutant cell lines was evaluated by their sensitivity to UVC (254 nm) and UVB (312 nm). Similar results were obtained for both wavelengths. $POLH^{-/-}$ cells were more sensitive than wild-type cells for both UV wavelengths (a 2-fold decrease in the D90 UV dose, achieving 90% cell mortality, fig. 3A, B & C). The UV sensitivity was not altered when these experiments were repeated with cells cultured in the presence of caffeine (data not shown). This result

was surprising since caffeine is known to exacerbate the sensitivity of human XPV fibroblasts to killing by UV [26]. However a caffeine-independent UV sensitivity has also been reported in chicken DT40 Pol η-deficient cells in which the P53 pathway is similarly inactive [27]. A full restoration of the resistance to UV light was obtained in two *POLH*$^{-/-}$ clones in which an expression vector encoding an EGFP-Pol η fusion protein was stably transfected (not shown). In parallel, the over-expression of Pol η in wild-type cells (more than 25-fold, see suppl. fig. 2), using tetracycline inducible expression vectors did not modify the resistance to UVB light (fig. 3C).

The *POLI*$^{-/-}$ was not UV sensitive, the survival curves being strictly identical to wild-type cells for both clones and both wavelengths. However BL2 cells deprived of both Pol η and Pol ι showed a higher sensitivity to UV-induced killing when compared to *POLH*$^{-/-}$ clones (a 1.6-fold decrease for the D90 value, fig. 3A). The inactivation of the *REV3L* gene in BL2 cell line led for both clones to the most drastic effect on UV-induced killing in all experiments, resulting in an increase in UV sensitivity of 10-fold when compared to wild-type cells (fig. 3A).

Analysis of the cell cycle after UV irradiation was performed in cells synchronized by incubation with 1 mM hydroxyurea. Sixteen hours after hydroxyurea addition, cells were UV-irradiated at 0.5, 2 or 4 J/m_ for *REV3L*$^{-/-}$, *POLH* $^{-/-}$ and wild-type cell lines respectively (an approximate D90 dose, allowing their comparison in similar conditions of UV-induced killing). Cell cycle was analyzed 24 h after irradiation by propidium iodide staining. The cell cycle was very differently affected: *POLH* $^{-/-}$ cells were predominantly blocked during their replication in the early S-phase of the cell cycle while *REV3L* $^{-/-}$ cells were largely blocked in a later S or early G2-phase (fig. 2B). Similar observations were made in asynchronous populations (Fig. 2A).

UV-dependent localization of EGFP-Pol η in POLI$^{-/-}$ *and REV3L*$^{-/-}$ *cell lines.*

Pol η has been shown to accumulate at DNA damage foci that form upon induction of replication blocking lesions. In XPV cells transiently transfected with EGFP-Pol η, the proportion of foci positive cells was largely increased after UV irradiation [28] We transfected an EGFP-Pol η construct in wild-type, Pol ι-deficient or REV3L-deficient cell lines. A stable transfection was preferred to a transient one to avoid the transfection stress and the risk of non physiological

expression. The different clones with the same genotype behaved similarly and the number of foci-positive cells reached a maximum 10h after irradiation (fig. 4A).

As shown in fig. 4B, the proportion of cells presenting spontaneous or UV-induced foci was largely increased on a REV3L-deficient background when compared to wild-type cells. This indicates that, in the absence of REV3L, Pol η accumulates at sites of endogenous DNA damage, the nature of which remains to be identified. Moreover it has been shown that Pol ι fails to accumulate efficiently at replication foci in Pol η-deficient cells [17]. In contrast, we observed that the absence of Pol ι had no impact on Pol η accumulation at replication foci after UV treatment.

The Pol η-deficient clone 123.12 was transfected with an EGFP-Pol η expression vector in which the PIP-box motif of the PCNA interacting domain was mutated: the four conserved amino acids within this motif at position 702-708 being mutated to alanines: QTLESFF [28, 29]. The transfected gene was expressed at a level comparable to wild-type in the 2 stable clones obtained (supplementary fig. 2 for the PIP-box mutant). The expression of the PIP-box mutant restored full UV resistance in these two clones (fig. 3B). However, they showed no replication foci 12h after UV irradiation (fig. 4A and 4B), thus indicating that functional complementation and accumulation at replication foci can be dissociated.

Mutant rate on UV-irradiated shuttle vector

The shuttle vector (pR2) is an SV40-based replicative plasmid, which contains the *lac*Z' target gene. It is cotransfected in BL2 cells with the pLAS vector, allowing the expression of SV40 T antigen, which is necessary for the bidirectional replication of pR2 from its SV40 origin of replication. The shuttle vector was irradiated *in vitro* with 3 kJ/m^2 of UVC and immediately cotransfected with pLAS in BL2. After 4 days, plasmids were collected and digested with *Dpn*I in order to eliminate non replicated copies. The digested DNA was transformed in *E.coli* and mutant rate at the *lac*Z' locus was determined using alpha-complementation (fig. 5). The spontaneous mutant rate on non-irradiated plasmids was below 0.7×10^{-3} with no significant differences observed between the cell lines. The shuttle experiment using irradiated plasmids was repeated at least three times in the different clones available for each cell line. As different clones with same genotype gave similar results, data were pooled.

In the two *POLH*$^{-/-}$ clones, mutagenesis induced by UVC was increased 1.5-fold compared to wild-type, as shown in fig. 5 ($P<0.05$ with Student test). The Pol ι deficiency had no impact on the mutant frequencies, whether on a Pol η proficient or-deficient background. On the contrary, the lack of REV3L decreased considerably the mutant rate on both clones (from 3.3 to 0.7%), but remained 10-fold higher than the spontaneous mutant rate (fig. 5).

Pattern of mutations induced by UV lesions

Table I summarizes mutations induced on the *lac*Z' gene after replication of UV-irradiated vector in the different polymerase-deficient cell lines. A total of 1246 mutations were collected, with only independent mutations being taken in consideration (suppl. fig. 3). Statistically significant differences, as determined by χ^2 tests, are marked in bold style in table I and are discussed below.

Point and tandems mutations:

UVC produced predominantly single base pair substitutions at pyrimidine dinucleotides sites in all the cell lines. As expected from the known mutagenic action of UV irradiation *in vivo*, most of the mutations were C to T transition events [30].

Misincorporations opposite the 3' position of TT sites were increased in both *POLH*$^{-/-}$ and *POLH*$^{-/-}$ *POLI*$^{-/-}$ cell lines, 39% and 32% respectively *vs*. 25% in wild-type. In contrast, the level of mutations at the 5'position of TT sites was significantly reduced (2% or less) in these cell lines compared to wild-type (6%), suggesting that Pol η might be occasionally mutagenic opposite the 5' position of TT sites.

The remaining mutations in the *REV3L*$^{-/-}$ background were mainly C to T transitions (89% *vs*. 42% in wild-type) occurring at the 3' position of TC and CC sites, with a shift in hotspot profile (see below). Strikingly, an increase in tandem CC to TT mutations (13% *vs*. 3%) was also noted in these cells. In parallel there was a drastic drop of mutations at the 3' position of TT (3% *vs*. 25% in wild-type) and CT sites (2% *vs*. 8 % in wild-type), showing clearly that Pol ζ is directly involved in misincorporations opposite UV damages containing thymines.

Double close mutations:

Some more complex mutations corresponding to two point mutations spaced by one correct base were frequently observed. The level of these "double close" mutations increased significantly in

POLH$^{-/-}$, *POLI*$^{-/-}$ and *POLH*$^{-/-}$ *POLI*$^{-/-}$ clones relative to the wild-type cell line. Interestingly, the wild-type nucleotide located between the two mutations was predominantly a thymidine residue, indicating that double close mutations arose from an error-prone bypass event in a 5'NTPy3' context (mutated nucleotides underlined). These mutations were completely absent in the *REV3L*$^{-/-}$ cell line indicating that these mutations are strictly REV3L-dependent.

Spectra of hotspot positions

Hotspots were determined according to the Poisson law, as described in materials and methods. Briefly, the position was considered as a hotspot if the amount of mutations at a given position was at least 4-fold above what a pure random mutagenesis would produce. When related to the mutation pool analyzed for each cell type, this represented 5 mutations for the wild-type, *POLI*$^{-/-}$ and *POLH*$^{-/-}$ *POLI*$^{-/-}$ cell lines, 7 for the *POLH*$^{-/-}$, and 4 for the *REV3L*$^{-/-}$ cell lines. The hotspots profiles for each cell line are shown in figure 6. All mutations scored are shown in supplementary figure 4.

Six additional hotspots occurred in the *POLH*$^{-/-}$ mutation spectrum (-38, 13, 43, 67, 68, 112) as compared to the wild-type profile, thus representing sites of UV damage for which the error-free bypass was strictly dependent on Pol η (fig. 6). Five of these hotspots disappeared in the *POLH*$^{-/-}$ *POLI*$^{-/-}$ mutation spectrum (-38, 13, 67, 68, 112), thus making likely that Pol ι is responsible for this mutagenic bypass in the absence of Pol η. These mutations were concentrated on TT dinucleotides in a 5' PuPyPyPu 3'context (3 out of 5, positions 13, 68 and 112), and notably for two of them in a 5'ATTA3'sequence. It has been demonstrated by *in vitro* TLS assays using purified proteins that Pol ι can catalyze error-prone bypass of TT CPDs located in such a 5'ATTA 3' sequence context [9]. Moreover, the mutation pattern of these 5 hotspots exhibited a higher frequency of transversions than the rest of the mutations (63% vs. 37%, p=0.0013, χ^2 test). For the position 43 hotspot, a polymerase other than Pol ι appears to be involved in mutagenesis when Pol η is absent, while error-free bypass requires Pol ζ.

In the *REV3L*$^{-/-}$ mutant background, cytosines were more targeted as evidenced by the presence of C targeted hotspots unique to this cell line at positions -69, 40, 76, 95 and 107.

Symmetrically, thymines were less targeted: three hotspots located on TT sites (positions 32, 73, and 98) were present in all but the *REV3L*$^{-/-}$ profile (fig. 6).

Complex mutations involving multiple TLS specificities

At position 71, 92 and 97, Pol η was mutagenic either alone (position 92) or in cooperation with REV3L (positions 71 and 97). In their absence, Pol ι alone could be used as an anti-mutagenic backup, since these hotspots were missing when Pol ι was expressed (fig. 6). A similar explanation applies to the hotspot at position -11, with the difference that, in the absence of both Pol η and Pol ι, error-prone bypass by a third polymerase (unknown) appears to take place. At position 127, a hotspot arose in the *POLI*$^{-/-}$ and the *REV3L*$^{-/-}$ spectra, suggesting that an error-free TLS was performed by the combined action of these two polymerases in wild-type cells. Finally, at position 47, a hotspot occurred in a *POLI*$^{-/-}$ and not in the double Pol η / Pol ι-deficient background implying that a mutagenic bypass by Pol η occurred in the absence of Pol ι. In all these cases, TLS could be aborted when Pol ι and Pol η are not present, since these hotspots were absent from the *POLI*$^{-/-}$ *POLH*$^{-/-}$ spectrum. Finally, hotspot mutations were observed at positions 31 and 80 in the double Pol η / Pol ι-deficient spectrum, suggesting that the simultaneous absence of these polymerases result in an error-prone bypass that does not require Pol ζ.

DISCUSSION

Human cell lines deficient in Pol η and Pol ι, either singly or in combination, or in REV3L, the catalytic subunit of Pol ζ, have been obtained by targeted inactivation of the corresponding genes, thus allowing for the first time the direct comparison of their respective phenotype in the same genetic background, the BL2 Burkitt's lymphoma.

The different deficient cell lines behaved differently when tested for their exponential growth and UV resistance. A slight increase in the doubling time was observed for the *POLH*$^{-/-}$ or the *POLI*$^{-/-}$ cell lines (22h instead of 20h), this increase being accentuated in the double deficient cell line (24h).

The growth retardation was still more pronounced in *REV3L*$^{-/-}$ cells with a doubling time of 29 h. This increase may be due to an increased cell loss by spontaneous cell death.

The Pol η-deficient clones were less resistant to UV irradiation than wild-type cells, while the *POLI*$^{-/-}$ cell line did not show any specific UV sensitivity. However BL2 cells deprived of both Pol η and Pol ι showed a marked increased sensitivity as compared to the Pol η-deficient cell line. It has been shown that adult fibroblasts derived from a Pol ι or a Pol ι/Pol η-deficient mouse were slightly more sensitive than their Pol ι proficient counterparts [19] but such an observation was not confirmed in MEF derived from a similar double deficient mouse [20]. The complete absence of the REV3L protein in the BL2 cell line led to the most drastic effect of UV-induced killing, resulting in a 7-fold increase in UV-sensitivity (estimated by the D90 values). Such an increased sensitivity after UV irradiation has been previously observed in a Rev3L-deficient mouse fibroblast cell line [31].

The analysis of the cell cycle after a mild irradiation revealed that the block in cell cycle progression occurred in late S or G2/M in *REV3L*$^{-/-}$ cell lines instead of early S for *POLH*$^{-/-}$ clones. In agreement with these results, XPV fibroblasts have been shown to be delayed in post-replicative repair after UV irradiation [26] whereas the REV3-deficient DT40 cell line was not [13]. A model for TLS has been recently re-actualized, based on bacterial and yeast data [32], proposing that replication can restart before complete lesion bypass is achieved, leaving gaps of single stranded DNA downstream the damaged DNA. Translating this model to higher eukaryotes, one could propose that Pol ζ would be required for sealing those gaps left by such replication restart process. The block in early-S cell cycle phase observed in Pol η-deficient cells after UV irradiation would suggest that replication restart could be conditioned by the initiation of lesion bypass. This proposition, obviously speculative, is detailed in supplementary figure 4.

A shuttle vector containing the *lac*Z' target gene and an SV40 origin of replication was transfected after irradiation in the different BL2 cell lines. The mutant rate of replicated plasmids determined at the *lac*Z' locus was increased by a factor of 1.5 in the Pol η-deficient cell lines as compared to wild-type cells. Increase in mutagenesis was similar in the double Pol η/Pol ι mutant cell line, but was not observed in the Pol ι only deficient background. In agreement with other

mutagenesis assays performed on chromosomal genes, there was a 4-fold drop in the frequency of mutations in the shuttle vector transfected in the two REV3L-deficient clones.

The shuttle approach allows the collection and analysis of large mutation datasets. Its inherent drawback lies in the partial chromatinization of the TLS substrate. Moreover, in these experiments, cells were not pre-irradiated prior to transfection of the shuttle vector. Nevertheless, the constitutive level of PCNA mono-ubiquitination observed in the BL2 cell line (our unpublished data) suggests that proper TLS complex may be assembled even in the absence of prior UV-irradiation of the transfected cells.

The large number of mutations collected in the present study allowed a detailed analysis of UV-induced mutations through the identification of hotspot positions whose occurrence reaches statistical significance. Some of these hotspots emerged in specific polymerase-deficient contexts, implying, along with the *in vitro* data, an *in vivo* bypass specificity for each of these polymerases.

Five specific mutation hotspots were only observed in the Pol η-deficient cell lines. These mutations, which disappeared in the Pol η/Pol ι-deficient cell line, were concentrated on TT sites (3 out of 5), and may thus be due to a back-up mutagenic bypass of TT CPDs by Pol ι[8, 19, 20, 33]. These hotspots show a specific mutation pattern with a predominant occurrence of transversions, in agreement with the mutation pattern of the *HPRT* gene observed in UV-irradiated fibroblasts of XPV patients and Pol η-deficient mice [19, 34]. However, we did not observe, after transfection of the shuttle vector in our *POLH*$^{-/-}$*POLI*$^{-/-}$ deficient cell line, the drop in mutation frequency described at the *HPRT* locus in two recent reports in which pol ι expression was either inactivated (mouse adult fibroblasts [19]), or simply reduced by anti-sense inhibition (transformed XPV fibroblasts) in a pol η-deficient context [33]. These differences are likely to reflect differences between irradiated episomal vectors and endogenous genes, or possibly between the cell type studied (lymphocytes *vs*. fibroblasts). Interestingly, three hotspots of mutation observed in the Pol ι deficient background suggest in contrast an anti-mutagenic lesion bypass activity of Pol ι.

In the absence of REV3L there was a marked drop in mutant frequency, indicating that about 4/5 of mutations found in wild-type cells are linked to Pol ζ activity. The remaining mutation pattern consisted mainly in C to T transitions targeted at the 3' C of TC and CC sites, and was correlated with

the presence of five hotspot positions unique to this cell line. A possible explanation for these mutations could be that replication over TC and CC photolesions may require Pol ζ as a bypass extender. In its absence, the slowing down of the process would result in an increase in cytosine deamination within photolesions, allowing for an unassisted synthesis in this new sequence configuration (TU or UU dimers) [35, 36]. This may explain how for example Pol η, which formed abundant UV-induced nuclear foci in the Pol ζ-deficient cell line (and also in the Pol ι-deficient cell line), could become mutagenic on such C-containing photolesions. Such a sequence of deamination events has been postulated to explain the P53 mutational pattern of C to T mutations within CPDs lesions in solar-induced human skin cancers [30]. Conversely mutations at the 3' T of TT and CT sites dropped considerably in the absence of REV3L, suggesting that such lesions could not be copied without Pol ζ. Accordingly, there were three mutation hotspots on TT dimers present in all cell lines at the exception of the Pol ζ-deficient one, pointing toward a role for Pol ζ, either alone or in association with another polymerase, in order to bypass these lesions.

There were again differences between the mutation pattern observed on the shuttle vector described in this study and the ones that have been scored at the *HPRT* locus in cell lines in which REV3L expression was reduced by an antisense transgene. However, in the two assays using anti-sense inhibition of REV3L expression in either mouse [37] or human fibroblasts [12], no UV-sensitivity was induced, in marked contrast to all other cases (mouse fibroblasts, DT40 and BL2) in which gene knock-out was performed, thus putting in question whether the impact of REV3L inactivation was really assessed.

While it has been shown that Pol ι does not efficiently participate in UV-induced nuclear foci in the absence of Pol η [17], our data and the ones published by other groups [19, 20, 33] tend nevertheless to indicate that Pol ι alone can be involved in damage tolerance at the replication fork. PCNA is mono-ubiquitinated in human cells after UV irradiation and it has been shown that this modification mediates its interaction with Pol η [38, 39]. Accordingly, Pol η and Pol ι only bind to mono-ubiquitinated PCNA. This binding occurs through two types of motifs, a PCNA interacting peptide (PIP-box motif), which binds directly to PCNA and provides the specificity of the reaction, and ubiquitin binding motifs (UBDs), which are strictly required for their accumulation at replication

factories [40]. Effectively, it has been reported that a Pol η PIP-box mutant could complement, although partially [40], the UV survival defect of an XPV fibroblast. Not only could we observe a complete restoration of UV resistance when the BL2 Pol η-deficient cell line was transfected with a Pol η PIP-box mutant but, much to our surprise, no UV-induced nuclear foci could be observed in this complemented cell line. These results on the UV resistance provided in a Pol η-deficient background by either Pol ι or a Pol η PIP-box mutant support the notion that TLS polymerases can be recruited at replication factories without the formation of observable UV-induced replication foci, the difference lying probably in their capacity to accumulate at sites of DNA damages beyond a detectable threshold.

Altogether these data strengthen, in a complete K.O. human model, the suggestion that Pol ι is involved in error-prone bypass of UV-induced lesions in the absence of Pol η, while also, and more surprisingly, being capable of error-free bypass in specific sequence contexts. These data also reinforce the notion that Pol ζ is a key partner in UV resistance and in the bypass of specific lesions, but also that this polymerase may be crucial for the maintenance of genome integrity during post-replicative repair. Moreover, the pattern of UV-induced mutations observed in the absence of Pol ζ with our shuttle vector strikingly mirrors the mutations observed in the TP53 gene from skin tumors which similarly display a strong C to T transition bias.

ACKNOWLEDGEMENTS

We thank E. Flatter, A. Van Der Linden, M. Ripaux and F. Delbos for their contribution to the establishment of polymerase-deficient cell lines, T. Honjo and M. Muramatsu for the gift of the pTet-tTAK-zeo vector and the transactivated BL2 cell line, A. Cordonnier for *in vitro* translesion assays, H. Mossafa for cytogenetic analysis and M. Garfa for assistance with confocal microscopy. This study was supported by the Ligue Nationale contre le Cancer (équipe labelisée). Q.G. was a fellow of Ligue Nationale contre le Cancer during part of this work.

REFERENCES:

[1] A.R. Lehmann, A. Niimi, T. Ogi, S. Brown, S. Sabbioneda, J.F. Wing, P.L. Kannouche, and C.M. Green, Translesion synthesis: Y-family polymerases and the polymerase switch, DNA Repair (Amst) (2007)
[2] E.C. Friedberg, A.R. Lehmann, and R.P. Fuchs, Trading places: how do DNA polymerases switch during translesion DNA synthesis?, Mol Cell 18 (2005) 499-505.
[3] R.E. Johnson, M.T. Washington, S. Prakash, and L. Prakash, Fidelity of human DNA polymerase η, J Biol Chem 275 (2000) 7447-7450.
[4] C. Masutani, M. Araki, A. Yamada, R. Kusumoto, T. Nogimori, T. Maekawa, S. Iwai, and F. Hanaoka, Xeroderma pigmentosum variant (XP-V) correcting protein from HeLa cells has a thymine dimer bypass DNA polymerase activity, Embo J 18 (1999) 3491-3501.
[5] R.E. Johnson, L. Haracska, S. Prakash, and L. Prakash, Role of DNA polymerase ζ in the bypass of a (6-4) TT photoproduct, Mol Cell Biol 21 (2001) 3558-3563.
[6] Y. Zhang, F. Yuan, X. Wu, J.S. Taylor, and Z. Wang, Response of human DNA polymerase ι to DNA lesions, Nucleic Acids Res 29 (2001) 928-935.
[7] R.E. Johnson, M.T. Washington, L. Haracska, S. Prakash, and L. Prakash, Eukaryotic polymerases ι and ζ act sequentially to bypass DNA lesions, Nature 406 (2000) 1015-1019.
[8] A. Tissier, E.G. Frank, J.P. McDonald, S. Iwai, F. Hanaoka, and R. Woodgate, Misinsertion and bypass of thymine-thymine dimers by human DNA polymerase ι, Embo J 19 (2000) 5259-5266.
[9] A. Vaisman, E.G. Frank, S. Iwai, E. Ohashi, H. Ohmori, F. Hanaoka, and R. Woodgate, Sequence context-dependent replication of DNA templates containing UV-induced lesions by human DNA polymerase ι, DNA Repair (Amst) 2 (2003) 991-1006.
[10] R.E. Johnson, C.M. Kondratick, S. Prakash, and L. Prakash, hRAD30 mutations in the variant form of xeroderma pigmentosum, Science 285 (1999) 263-265.
[11] C. Masutani, R. Kusumoto, A. Yamada, N. Dohmae, M. Yokoi, M. Yuasa, M. Araki, S. Iwai, K. Takio, and F. Hanaoka, The XPV (xeroderma pigmentosum variant) gene encodes human DNA polymerase eta, Nature 399 (1999) 700-704.
[12] P.E. Gibbs, W.G. McGregor, V.M. Maher, P. Nisson, and C.W. Lawrence, A human homolog of the Saccharomyces cerevisiae REV3 gene, which encodes the catalytic subunit of DNA polymerase ζ, Proc Natl Acad Sci U S A 95 (1998) 6876-6880.
[13] E. Sonoda, T. Okada, G.Y. Zhao, S. Tateishi, K. Araki, M. Yamaizumi, T. Yagi, N.S. Verkaik, D.C. van Gent, M. Takata, and S. Takeda, Multiple roles of Rev3, the catalytic subunit of pol ζ in maintaining genome stability in vertebrates, Embo J 22 (2003) 3188-3197.
[14] M. Bemark, A.A. Khamlichi, S.L. Davies, and M.S. Neuberger, Disruption of mouse polymerase ζ (Rev3) leads to embryonic lethality and impairs blastocyst development in vitro, Curr Biol 10 (2000) 1213-1216.
[15] G. Esposito, I. Godindagger, U. Klein, M.L. Yaspo, A. Cumano, and K. Rajewsky, Disruption of the Rev3l-encoded catalytic subunit of polymerase ζ in mice results in early embryonic lethality, Curr Biol 10 (2000) 1221-1224.
[16] J. Wittschieben, M.K. Shivji, E. Lalani, M.A. Jacobs, F. Marini, P.J. Gearhart, I. Rosewell, G. Stamp, and R.D. Wood, Disruption of the developmentally regulated Rev3l gene causes embryonic lethality, Curr Biol 10 (2000) 1217-1220.
[17] P. Kannouche, A.R. Fernandez de Henestrosa, B. Coull, A.E. Vidal, C. Gray, D. Zicha, R. Woodgate, and A.R. Lehmann, Localization of DNA polymerases η and ι to the replication machinery is tightly co-ordinated in human cells, Embo J 22 (2003) 1223-1233.

[18] J.H. Choi, A. Besaratinia, D.H. Lee, C.S. Lee, and G.P. Pfeifer, The role of DNA polymerase ι in UV mutational spectra, Mutat Res 599 (2006) 58-65.
[19] C.A. Dumstorf, A.B. Clark, Q. Lin, G.E. Kissling, T. Yuan, R. Kucherlapati, W.G. McGregor, and T.A. Kunkel, Participation of mouse DNA polymerase ι in strand-biased mutagenic bypass of UV photoproducts and suppression of skin cancer, Proc Natl Acad Sci U S A 103 (2006) 18083-18088.
[20] T. Ohkumo, Y. Kondo, M. Yokoi, T. Tsukamoto, A. Yamada, T. Sugimoto, R. Kanao, Y. Higashi, H. Kondoh, M. Tatematsu, C. Masutani, and F. Hanaoka, UV-B radiation induces epithelial tumors in mice lacking DNA polymerase η and mesenchymal tumors in mice deficient for DNA polymerase ι, Mol Cell Biol 26 (2006) 7696-7706.
[21] C. Capoulade, B. Bressac-de Paillerets, I. Lefrere, M. Ronsin, J. Feunteun, T. Tursz, and J. Wiels, Overexpression of MDM2, due to enhanced translation, results in inactivation of wild-type p53 in Burkitt's lymphoma cells, Oncogene 16 (1998) 1603-1610.
[22] C. Marionnet, A. Benoit, S. Benhamou, A. Sarasin, and A. Stary, Characteristics of UV-induced mutation spectra in human XP-D/ERCC2 gene-mutated xeroderma pigmentosum and trichothiodystrophy cells, J Mol Biol 252 (1995) 550-562.
[23] A. Faili, S. Aoufouchi, E. Flatter, Q. Gueranger, C.A. Reynaud, and J.C. Weill, Induction of somatic hypermutation in immunoglobulin genes is dependent on DNA polymerase ι, Nature 419 (2002) 944-947.
[24] C.M. Kondratick, M.T. Washington, S. Prakash, and L. Prakash, Acidic residues critical for the activity and biological function of yeast DNA polymerase η, Mol Cell Biol 21 (2001) 2018-2025.
[25] R. Redon, S. Ishikawa, K.R. Fitch, L. Feuk, G.H. Perry, T.D. Andrews, H. Fiegler, M.H. Shapero, A.R. Carson, W. Chen, E.K. Cho, S. Dallaire, J.L. Freeman, J.R. Gonzalez, M. Gratacos, J. Huang, D. Kalaitzopoulos, D. Komura, J.R. MacDonald, C.R. Marshall, R. Mei, L. Montgomery, K. Nishimura, K. Okamura, F. Shen, M.J. Somerville, J. Tchinda, A. Valsesia, C. Woodwark, F. Yang, J. Zhang, T. Zerjal, J. Zhang, L. Armengol, D.F. Conrad, X. Estivill, C. Tyler-Smith, N.P. Carter, H. Aburatani, C. Lee, K.W. Jones, S.W. Scherer, and M.E. Hurles, Global variation in copy number in the human genome, Nature 444 (2006) 444-454.
[26] A.R. Lehmann, S. Kirk-Bell, C.F. Arlett, M.C. Paterson, P.H. Lohman, E.A. de Weerd-Kastelein, and D. Bootsma, Xeroderma pigmentosum cells with normal levels of excision repair have a defect in DNA synthesis after UV-irradiation, Proc Natl Acad Sci U S A 72 (1975) 219-223.
[27] T. Kawamoto, K. Araki, E. Sonoda, Y.M. Yamashita, K. Harada, K. Kikuchi, C. Masutani, F. Hanaoka, K. Nozaki, N. Hashimoto, and S. Takeda, Dual roles for DNA polymerase η in homologous DNA recombination and translesion DNA synthesis, Mol Cell 20 (2005) 793-799.
[28] P. Kannouche, B.C. Broughton, M. Volker, F. Hanaoka, L.H. Mullenders, and A.R. Lehmann, Domain structure, localization, and function of DNA polymerase η, defective in xeroderma pigmentosum variant cells, Genes Dev 15 (2001) 158-172.
[29] L. Haracska, R.E. Johnson, I. Unk, B. Phillips, J. Hurwitz, L. Prakash, and S. Prakash, Physical and functional interactions of human DNA polymerase η with PCNA, Mol Cell Biol 21 (2001) 7199-7206.
[30] G. Giglia-Mari and A. Sarasin, TP53 mutations in human skin cancers, Hum Mutat 21 (2003) 217-228.
[31] J.P. Wittschieben, S.C. Reshmi, S.M. Gollin, and R.D. Wood, Loss of DNA polymerase zeta causes chromosomal instability in mammalian cells, Cancer Res 66 (2006) 134-142.

[32] A.R. Lehmann and R.P. Fuchs, Gaps and forks in DNA replication: Rediscovering old models, DNA Repair (Amst) 5 (2006) 1495-1498.
[33] Y. Wang, R. Woodgate, T.P. McManus, S. Mead, J.J. McCormick, and V.M. Maher, Evidence that in xeroderma pigmentosum variant cells, which lack DNA polymerase η, DNA polymerase ι causes the very high frequency and unique spectrum of UV-induced mutations, Cancer Res 67 (2007) 3018-3026.
[34] Y.C. Wang, V.M. Maher, D.L. Mitchell, and J.J. McCormick, Evidence from mutation spectra that the UV hypermutability of xeroderma pigmentosum variant cells reflects abnormal, error-prone replication on a template containing photoproducts, Mol Cell Biol 13 (1993) 4276-4283.
[35] D.H. Lee and G.P. Pfeifer, Deamination of 5-methylcytosines within cyclobutane pyrimidine dimers is an important component of UVB mutagenesis, J Biol Chem 278 (2003) 10314-10321.
[36] A. Stary, P. Kannouche, A.R. Lehmann, and A. Sarasin, Role of DNA polymerase η in the UV mutation spectrum in human cells, J Biol Chem 278 (2003) 18767-18775.
[37] M. Diaz, N.B. Watson, G. Turkington, L.K. Verkoczy, N.R. Klinman, and W.G. McGregor, Decreased frequency and highly aberrant spectrum of ultraviolet-induced mutations in the hprt gene of mouse fibroblasts expressing antisense RNA to DNA polymerase ζ, Mol Cancer Res 1 (2003) 836-847.
[38] P.L. Kannouche, J. Wing, and A.R. Lehmann, Interaction of human DNA polymerase η with monoubiquitinated PCNA: a possible mechanism for the polymerase switch in response to DNA damage, Mol Cell 14 (2004) 491-500.
[39] K. Watanabe, S. Tateishi, M. Kawasuji, T. Tsurimoto, H. Inoue, and M. Yamaizumi, Rad18 guides pol η to replication stalling sites through physical interaction and PCNA monoubiquitination, Embo J 23 (2004) 3886-3896.
[40] M. Bienko, C.M. Green, N. Crosetto, F. Rudolf, G. Zapart, B. Coull, P. Kannouche, G. Wider, M. Peter, A.R. Lehmann, K. Hofmann, and I. Dikic, Ubiquitin-binding domains in Y-family polymerases regulate translesion synthesis, Science 310 (2005) 1821-1824.

FIGURE LEGENDS:

Fig. 1: Scheme of the homologous recombination strategy used to inactivate the *POLH* (A) or the *REV3L* gene (B).

Non coding exons are indicated in white rectangles and coding exons in black rectangles, with resistance cassette not drawn at scale. The *POLH* locus extends over 39.5 kbp and *REV3L* over 184 kbp. Scale bars are 5 kbp wide. (a): constructs used to inactivate *POLH* in the wild-type BL2 cell line. (b): constructs used to inactivate *POLH* in a *POLI* $^{-/-}$ cell line. Resistance names written upside down are in reverse orientation compared to the loci.

Fig. 2: Cell cycle analysis in polymerase-deficient cell lines.

A) Cell cycle analysis of UV-irradiated and control cells. Cells were incubated during 4 h with BrdU prior to analysis with propidium iodide and anti-BrdU antibody staining. The analysis was performed

on unirradiated cells (upper panel) or 20h after UV irradiation corresponding to the D90 value of each cell line (lower panel). B) Cell cycle analysis of synchronized wt, Pol η and Pol ζ-deficient cells after UV irradiation. Cells were synchronized in early S phase by 16 h incubation with 1 mM hydroxyurea. Cells were UV-irradiated immediately after drug removal with doses corresponding to D90 values (given in the legend of the fig. 3), and their cell cycle analyzed 24 h later by propidium iodide staining.

Fig. 3: Survival of cell lines exposed to UV light.

Survival is expressed in percentage of non-irradiated control.

A) UV sensitivity of the WT, *POLH* $^{-/-}$, *POLI* $^{-/-}$, double deficient and *REV3L*$^{-/-}$ cell lines. All cell lines were irradiated simultaneously. B) Restoration of UV resistance in a Pol η-deficient clone by expression of an EGFP Pol η PIP-box mutant. C) Restoration of UV resistance in a Pol η-deficient clone by wt EGFP Pol η overexpression. A, B) UVC irradiation. C) UVB irradiation. D90 doses (J/m_ UVC): 4.22±0.38 for WT cells, calculated on the basis of n=10 experiments; 2.05±0.35 for Pol η-deficient cells (n=23); 4.1±0.4 for Pol ι-deficient cells (n=7); 1.27±0.28 for Pol η Pol ι-deficient cells (n=15); 0.42±0.2 for REV3L-deficient cells (n= 8).

Fig. 4: Accumulation of EGFP-Pol η in replication foci.

EGFP-Pol η was stably expressed in wt, Pol ι and REV3L-deficient cell lines and an EGFP-Pol η PIP-box mutant was stably expressed in the Pol η-deficient cell line. A) Representative confocal images of BL2 polymerase-deficient cell lines with or without UV irradiation (10 J/m_ of UVC).

B) Proportion of EGFP-Pol η foci-positive cells in different polymerase-deficient backgrounds. Mean values and range of three independent experiments are represented.

Fig. 5: Mutant frequencies of the *lac*Z' gene of the UV-irradiated shuttle vector.

Frequencies are calculated by the proportion of light blue / white colonies relative to dark blue ones after transformation in *E.coli*. Each mutant was checked by sequencing. Mean value and error bars of 3 independent experiments are represented for each cell line.

Fig. 6: Hotspot positions along the *lac*Z' gene of the UV-irradiated shuttle vector.

Numbers refer to the *lac*Z' sequence with 1 being the ATG initiator codon. Only hotspots that reached a statistically significant threshold are shown (see definition in Materials and Methods). The complete representation of collected mutations is shown in supplementary fig.4. The red bars indicate hotspots restricted to specific polymerase contexts. Blue arrows indicate a position where a specific hotspot is missing. In both cases, these hotspots are written within a 5 nucleotide sequence context with the mutated nucleotide underlined. The peak height is proportional to the percentage of hotspot mutations at any given position (the bar scale represents 10 % of hotspot mutations).

Supplementary fig. 1: Control of *POLH, POLI* and *REV3L* inactivation.

A) *POLH*$^{-/-}$ and *POLI*$^{-/-}$*POLH*$^{-/-}$ cell lines were checked by western blot for the absence of the Pol η.

B) The absence of REV3L mRNA in the two *REV3L*$^{-/-}$ clones was checked by RT-PCR.

Supplementary fig. 2: Pol η expression during the PIP-box mutant restoration experiment (lane 6) and the overexpression experiment in wt cells (lane 8). PCNA is used for normalization.

Supplementary fig. 3: Distribution of all scored mutations along the *lac*Z' target gene.

Tandem mutations are highlighted in yellow, ''double close'' mutations are highlighted in red. Insertions are marked with a (+) over the previous nucleotide and deletions are indicated by dashes. Numbering refers to the sequence of the *lac*Z', 1 being the first base of the ATG initiator codon.

Supplementary fig. 4: A hypothetical scheme for a replication restart model involving pol ζ in a gap filling process.

Replication restart would occur when the replication fork encounters UV damage in the wt and *REV3L*$^{-/-}$ context, allowing the cell to proceed up to the G2 phase and to perform post-replicative repair (PRR) as monitored by ^{3}H-thymidine pulse-chase labeling (in blue on the scheme). Filling of gaps left behind the replication fork would be performed or initiated by Pol ζ (in green). *REV3L*$^{-/-}$ cells would be accordingly blocked in G2. No replication restart would occur in Pol η-deficient cells,

which are blocked in early S and show delayed PRR, thus implying that replication restart might be conditioned to the engagement of Pol η opposite the UV lesion (in red).

Table I: Mutation profile of the irradiated shuttle vector after replication in the various polymerase-deficient cell lines.

	cell type	WT	*POLH*$^{-/-}$	*POLI*$^{-/-}$	*POLI*$^{-/-}$ *POLH*$^{-/-}$	*REV3L*$^{-/-}$
	Number of clones		2	2	1	2
	Number of experiments	4	7	4	4	6
Type of mutation (%)	Single substitutions	79	80	77	82	82
	CC to TT tandems	4	2	3	3	**13***
	Other tandems	12	8	8	7	**1****
	Double close	3	**9****	**9****	**7***	0
	Frameshifts	2	1	3	2	3
	Deletions	1	0	0	0	1
Overall mutation pattern (%)	C to T	42	40	47	43	**89*****
	C to A	11	9	9	11	**1*****
	C to G	4	2	5	1	3
	T to C	17	20	16	19	**6****
	T to A	19	23	17	16	**1*****
	T to G	7	6	6	10	**1*****
Mutation targeting (%)	T<u>T</u> 3'	25	**39****	25	32	**3****
	T<u>C</u> 3'	40	38	31	37	59
	C<u>T</u> 3'	8	6	10	9	2
	C<u>C</u> 3'	15	9	14	13	22
	5'<u>T</u>T	6	**2***	6	**1***	3
	5'<u>T</u>C	1	0	1	1	0
	5'<u>C</u>T	2	1	1	2	6
	5'<u>C</u>C	0	0	2	1	0
	Non di-pyrimidic	4	4	**10***	4	6

All values are expressed in percentage of the total number of mutations indicated at the bottom of each section. T<u>T</u> 3' indicates that the mutation occurred opposite the 3' position of the dinucleotide. On the contrary, 5'<u>T</u>T indicates that replication was error prone opposite the 5' nucleotide. Tandem mutations are scored as 2 mutations. * marks P value <0.05, ** P<0.01 and *** P<0.001 as determined by the χ^2 test. Total number of mutation analyzed: WT n=220, *POLH*$^{-/-}$ n=407, *POLI*$^{-/-}$ n=228, *POLI*$^{-/-}$ *POLH*$^{-/-}$ n=238, *REV3L*$^{-/-}$ n=153.

Figure 1

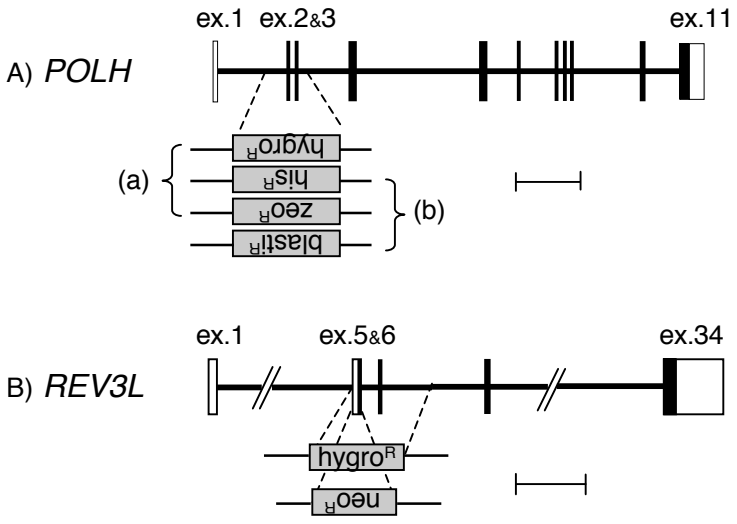
ex.1
ex.2&3
ex.11
A) POLH
(a)
hygroR
hisR
zeoR
blastiR
(b)
ex.1
ex.5&6
ex.34
B) REV3L
hygroR
neoR

Figure 2

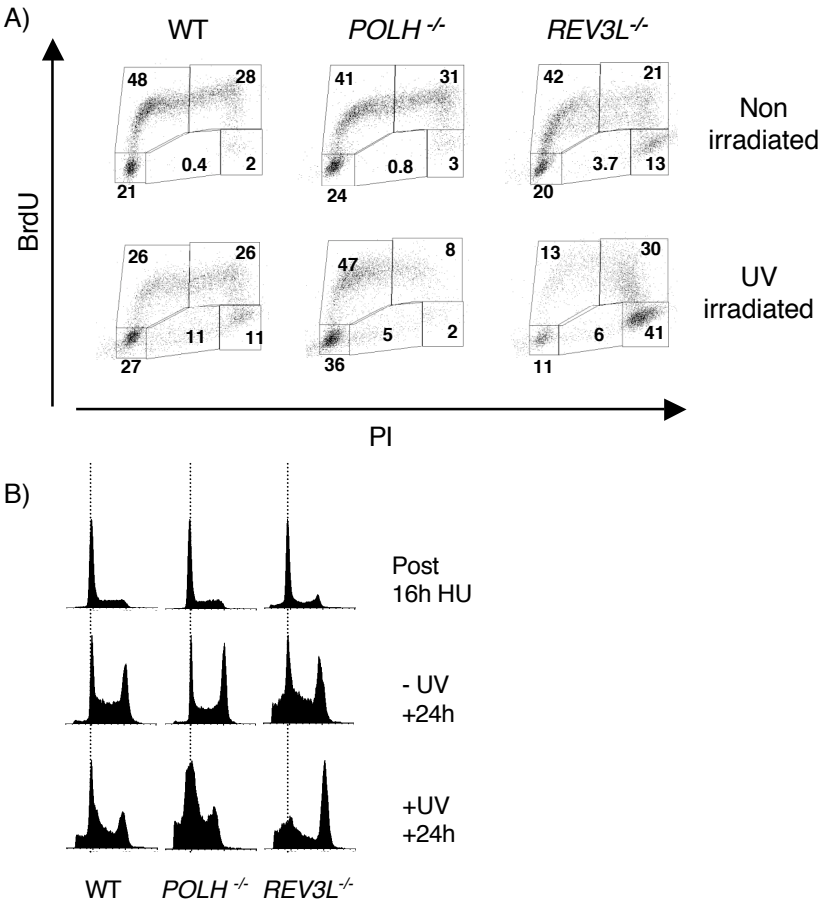
A)
WT
POLH -/-
REV3L-/-
48
28
0.4
2
21
41
31
0.8
3
24
42
21
3.7
13
20
Non irradiated
26
26
11
11
27
47
8
5
2
36
13
30
6
41
11
UV irradiated
BrdU
PI
B)
Post 16h HU
- UV +24h
+UV +24h
WT
POLH -/-
REV3L-/-

Figure 3

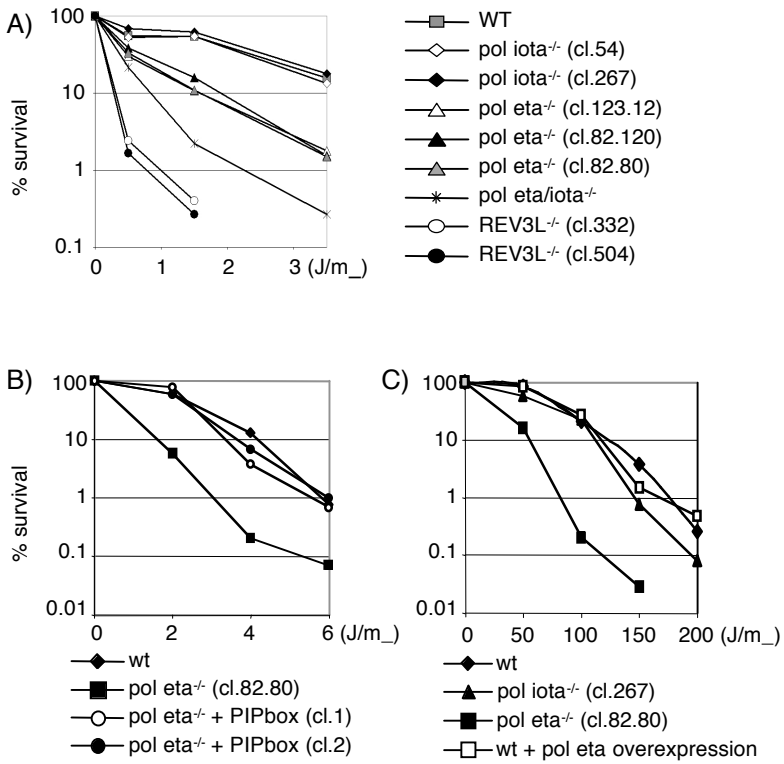
A)
100
10
1
0.1
% survival
0
1
2
3 (J/m_)
WT
pol iota-/- (cl.54)
pol iota-/- (cl.267)
pol eta-/- (cl.123.12)
pol eta-/- (cl.82.120)
pol eta-/- (cl.82.80)
pol eta/iota-/-
REV3L-/- (cl.332)
REV3L-/- (cl.504)
B)
100
10
1
0.1
0.01
% survival
0
2
4
6 (J/m_)
wt
pol eta-/- (cl.82.80)
pol eta-/- + PIPbox (cl.1)
pol eta-/- + PIPbox (cl.2)
C)
100
10
1
0.1
0.01
0
50
100
150
200 (J/m_)
wt
pol iota-/- (cl.267)
pol eta-/- (cl.82.80)
wt + pol eta overexpression

Figure 4

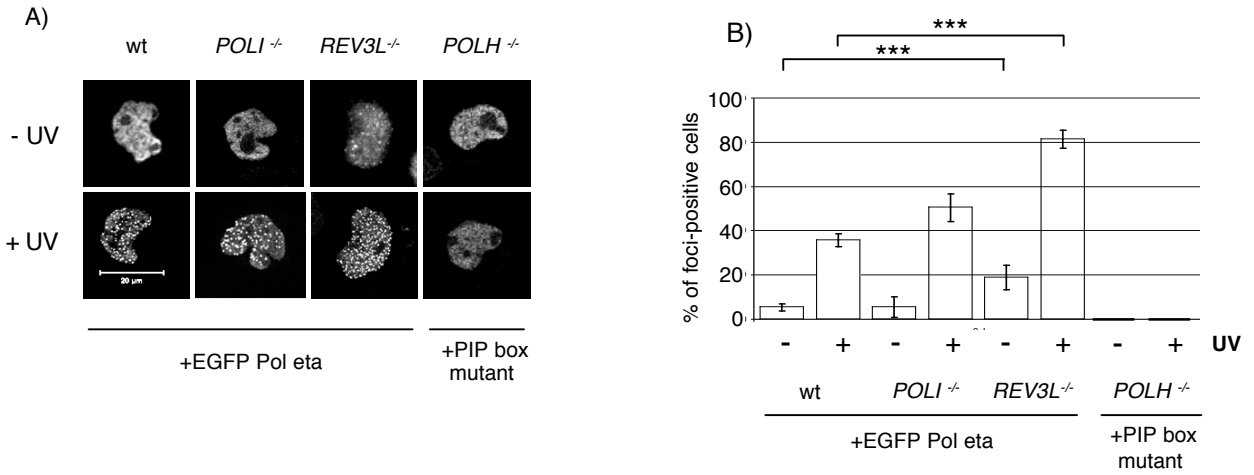
A)
wt
POLI -/-
REV3L-/-
POLH -/-
- UV
+ UV
20 µm
+EGFP Pol eta
+PIP box mutant
B)
***
***
% of foci-positive cells
100
80
60
40
20
0
- + - + - + - + UV
wt
POLI -/-
REV3L-/-
POLH -/-
+EGFP Pol eta
+PIP box mutant

Figure 5

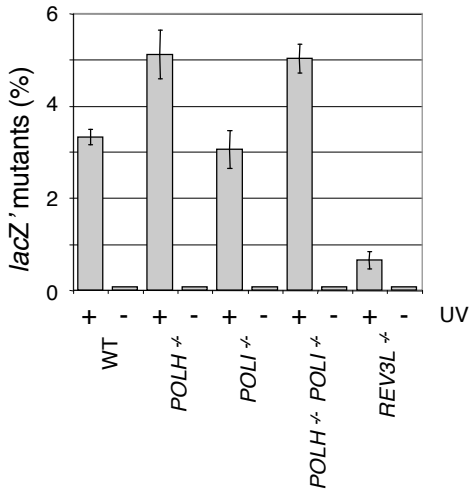

Figure 6

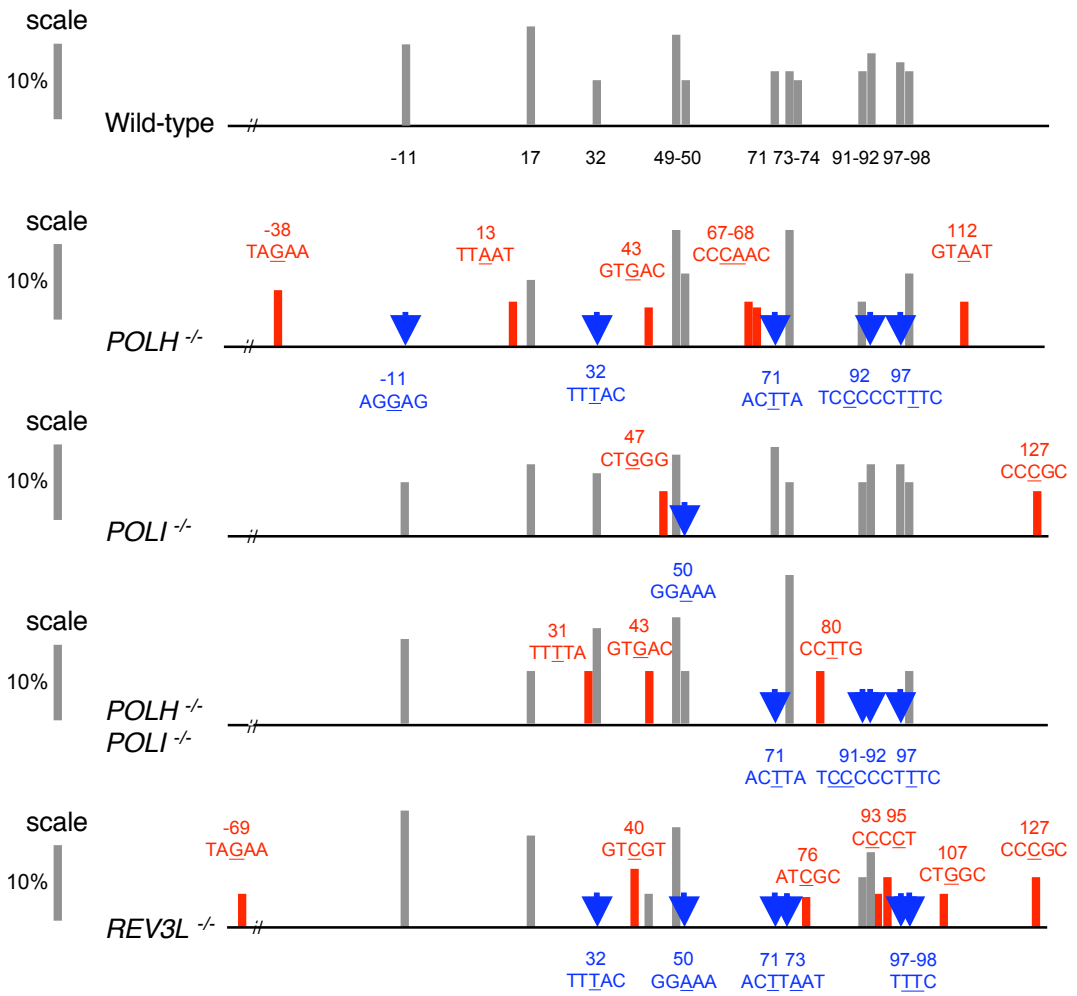
scale
10%
Wild-type
-11
17
32
49-50
71 73-74
91-92 97-98
POLH -/-
-38 TAGAA
13 TTAAT
43 GTGAC
67-68 CCCAAC
112 GTAAT
-11 AGGAG
32 TTTAC
71 ACTTA
92 TCCCCCTTTC
97
POLI -/-
47 CTGGG
127 CCCGC
POLH -/-
POLI -/-
50 GGAAA
31 TTTTA
43 GTGAC
80 CCTTG
71 ACTTA
91-92 TCCCCCTTTC
97
REV3L -/-
-69 TAGAA
40 GTCGT
76 ATCGC
93 95 CCCCT
107 CTGGC
127 CCCGC
32 TTTAC
50 GGAAA
71 73 ACTTAAT
97-98 TTTC

Supplementary figure 1

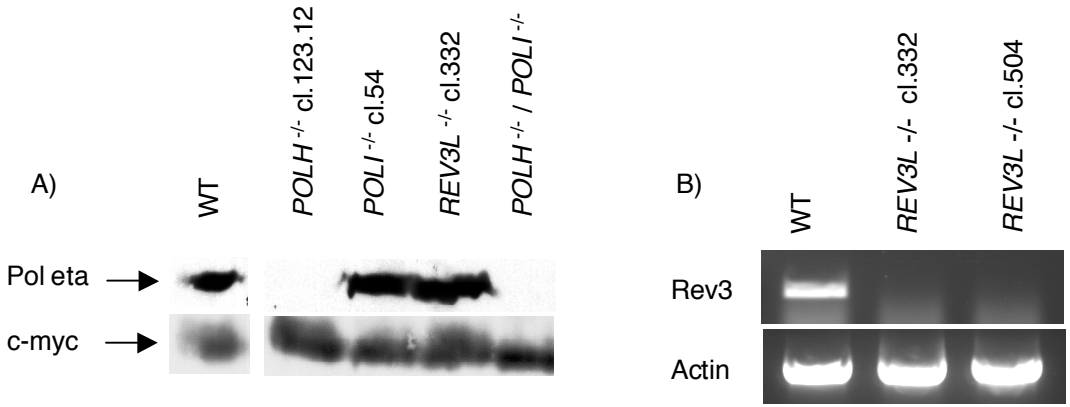

Supplementary figure 2

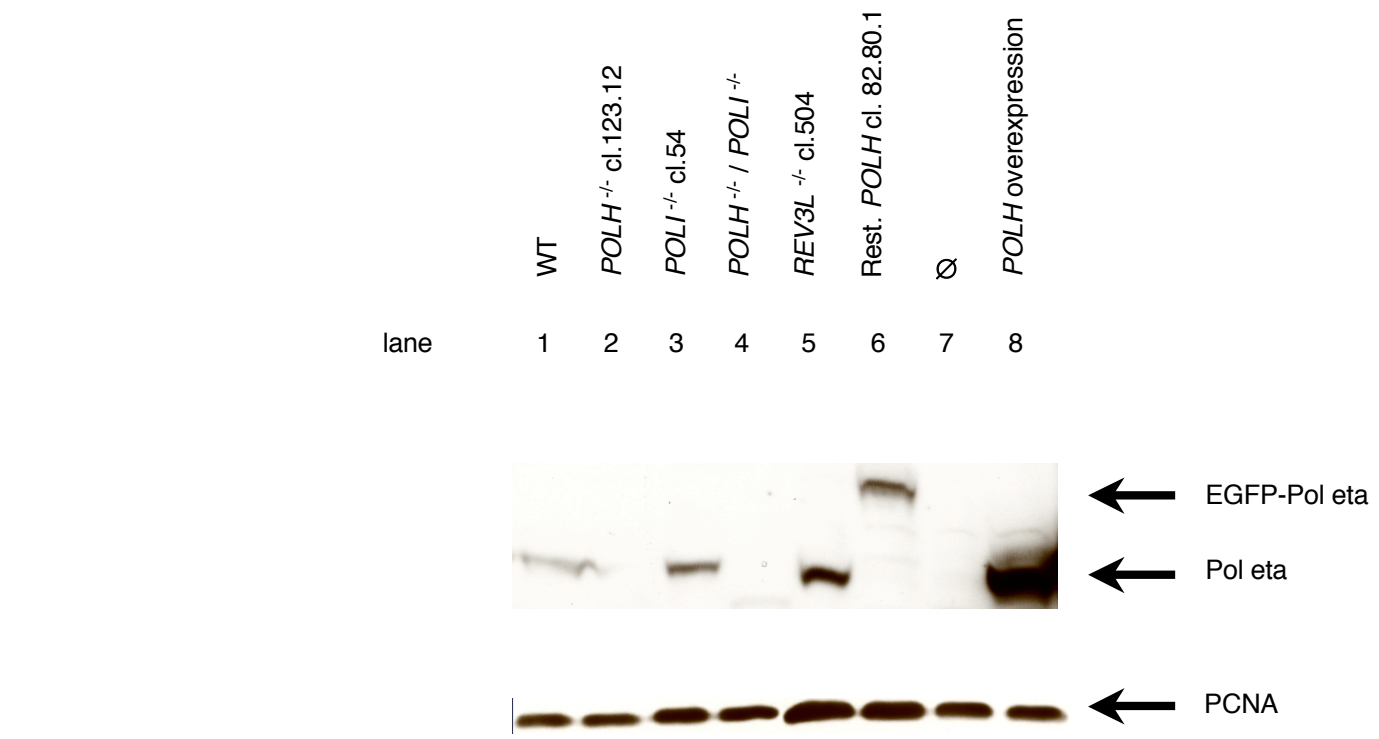

Supplementary figure 3

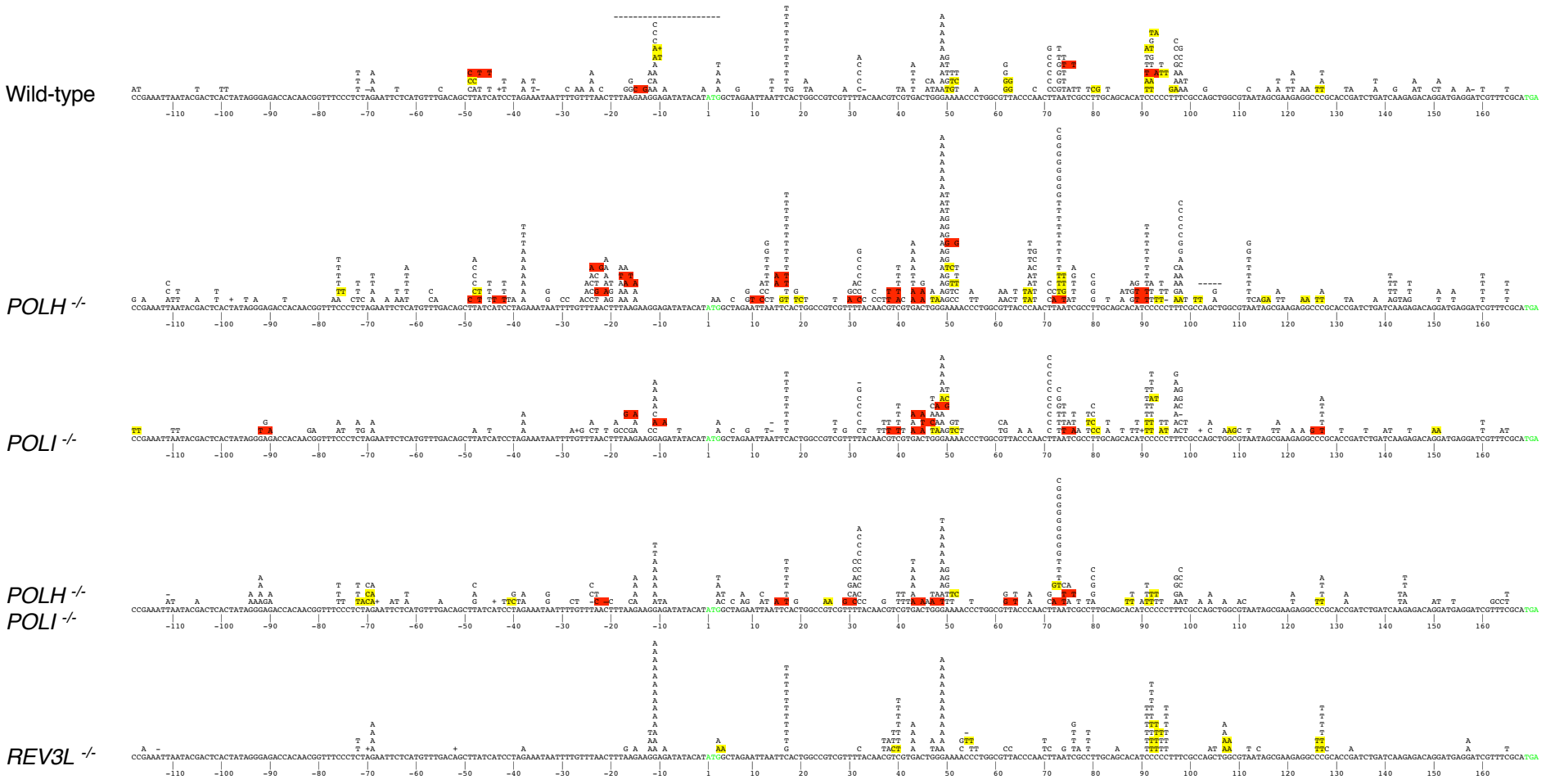

Supplementary figure 4